Phosphonium polymethacrylates for siRNA delivery: effect of polymer and RNA structural parameters on polyplex assembly and gene knockdown.

Vanessa Loczenski Rose[a], Saif Shubber[a], S. Sajeesh[b], Sebastian G. Spain[c], Sanyogitta Puri[d], Stephanie Allen[a], Dong-Ki Lee[b], G. Sebastiaan Winkler[a], and Giuseppe Mantovani[a]**

[a]School of Pharmacy, Boots Science Building, University Park, University of Nottingham, Nottingham, NG7 2RD, UK

[b]Global Research Laboratory for RNAi Medicine, Department of Chemistry, Sungkyunkwan University, Suwon 440-746, Republic of Korea

[c]Department of Chemistry, Dainton Building, University of Sheffield, Sheffield, S3 7HF, UK

[d]Astrazeneca UK Ltd., Pharmaceutical Development, Alderley Park, Macclesfield SK10 2NA, UK

ABSTRACT: Synthetic polymers containing quaternary phosphonium salts are an emerging class of materials for the delivery of oligo/polynucleotides. In this work, cationic phosphonium salt-containing polymethacrylates –and their corresponding ammonium analogues– were synthesized by RAFT polymerization. Both the nature of the charged heteroatom (N vs. P) and the length of the spacer separating the cationic units along the polymer backbone (oxyethylene vs. trioxyethylene) were systematically varied. Polymers efficiently bound siRNA at N^+/P^- or P^+/P^- ratios of 2 and above. At a 20:1 ratio, small polyplexes (R_h: 4-15 nm) suitable for cellular uptake were formed that displayed low cytotoxicity. Whilst siRNA polyplexes from both ammonium and phosphonium polymers were efficiently internalised by GFP-expressing 3T3 cells, no knockdown of GFP expression was observed. However, 65% Survivin gene knockdown was observed when short interfering RNA (siRNA) was replaced with novel, multimerised long interfering liRNA

(liRNA) in HeLa cells, demonstrating the importance of RNA macromolecular architecture on RNA-mediated gene silencing.

INTRODUCTION

Over the past few years RNA interference (RNAi) mediated by double stranded RNA has gained enormous attention as a potential therapeutic strategy to treat currently undruggable diseases[1–3]. However, the delivery of RNA to the desired target organ as well as the control over intracellular trafficking remains a major challenge currently limiting the technology. Various strategies for RNA delivery have been explored, such as the application of lipid-based delivery systems (lipoplexes and liposomes)[4–6], nanoparticles[7–9], viruses[10], peptide-based systems[7], polymers[11–14] and gold-based materials[15–18].

Polymer-based delivery systems offer the potential advantages of scalability, increased safety and flexibility to introduce modifications post polymerization for targeted delivery[19]. Recent advances in controlled radical polymerization (CRP) provide unprecedented control over monomer sequence[20,21], chemical functionalities[22,23] and molecular weight distribution[24–26]. CRP has been extensively utilized for the synthesis of polymers suitable for biological applications such as nucleic acid delivery systems[25,27–34]. Covalent and non-covalent RNA-polymer conjugation approaches have been described[35]. The latter strategy, where polymer-nucleic acid complexes (polyplexes) are generated via ionic interactions between cationic polymers and negatively charged RNA has been more frequently investigated. Whilst nitrogen-containing cationic polymers such as *N,N*-dimethylaminoethyl methacrylate (DMAEMA), polyethylenimine (PEI), poly(l-lysine) and others are commonly used[36,37], polymers incorporating phosphonium salt functionalities have recently started to gain interest as novel materials with a range of properties complementing existing nitrogen-based systems[38–44]. Phosphonium-containing polymers have been engineered with reduced cytotoxicity and efficient binding of oligonucleotides, at least in

part due to the different ionic radius and charge distribution of quaternary phosphonium salts compared to their corresponding ammonium counterparts[38–40]. However, the application of phosphonium polymers in oligo/polynucleotide delivery is to date still limited, with only few phosphonium based monomers readily available. A significant challenge in this has been the identification of appropriate synthetic routes, additional cost of starting materials, and air-sensitive and often pyrophoric nature of the organic phosphine precursors required for their preparation.

In the present study we report a novel synthetic route for a new class of cationic polymethacrylates. This involved the synthesis of water soluble, phosphonium containing methacrylate monomers – and their corresponding ammonium analogues - and subsequent aqueous RAFT polymerization. The resulting methacrylate polymers were characterized with regards to their physicochemical properties and suitability as RNA delivery systems. The influence of polymer structural parameters such as the nature of the charged heteroatom (N vs P) and the length of the spacer connecting the later to the polymer backbone were investigated. In addition, the impact on gene knockdown of the molecular architecture of RNA was evaluated.

EXPERIMENTAL SECTION

Materials: Chemicals and reagents were purchased at the highest purity available from Sigma-Aldrich unless otherwise stated and were used as received without purification. All solvents were bought from Fisher Scientific. Yields of monomers and intermediates were not optimized. Cell reagents were purchased from Life Technologies, unless stated otherwise. siRNA duplexes for gel retardation assays and GFP knockdown studies were purchased from Dharmacon (siGENOME Non-Targeting siRNA #2 and GFP Duplex I, P-002048-01); siRNA for cellular uptake studies was purchased from Qiagen (AllStars negative siRNA Alexa Fluor 647). liRNA containing the

following sequence: 5' UGAAAAUGUUGAUCUCCUUUCCUAAGACAUUGCUAAGG 3' and 3' AGGAUUCUGUAACGAUUCCACUUUUACAACUAGAGGAA 5' was purchased from ST Pharm (Seoul, Korea) and multimerized. Interferin was obtained from Polyplus transfection. Primers for reverse transcriptase PCR were purchased from Daejeon (Korea): GAPDH forward 5' GACTCAACGGATTTG GTC GT 3', GAPDH reverse 5'GACAAGCTTCCCGTTCTCAG 3', Survivin forward 5'GCACCACTTCCAGGGTTTAT 3', Survivin reverse 5' CTCTGGTGCCACTTTCAAGA 3';

Analysis: Mass spectrometry (MS) was performed using a Waters 2795 separation module/micromass LCT platform. Samples were mixed with 200 µl of acetonitrile + 0.1% formic acid and 200 µl of water + 0.1% formic acid and analyzed immediately.

Nuclear magnetic resonance (NMR) spectra were acquired with a Bruker DPX UltraShield spectrometer at 25°C. Samples (^{1}H NMR, ^{13}C NMR, ^{31}P NMR) were prepared in deuterated solvents ($CDCl_3$, D_2O or DMSO-d_6, Methanol-d_4) and chemical shifts were reported in parts per million (ppm) with reference to solvent residual peaks or tetramethylsilane (TMS). Coupling constants were reported in Hertz (Hz). Spectra were collected following frequencies: 400 MHz (^{1}H), 100 MHz (^{13}C) and 161.9 MHz (^{31}P). Spectra were processed using Mestrenova software 6.0.2. Fourier transform infrared spectroscopy (FT-IR) was performed with an Agilent Cary 630 FTIR spectrometer.

***N,N,N*-triethyl-2-(methacryloyloxy)ethan-1-aminium chloride (3a):** Monomer **3a** was prepared in a 2 step reaction process. Firstly, 2-bromoethanol (35.3 g, 280 mmol) and Et_3N (42.8 g, 423 mmol) in toluene (100 ml) were heated at 75°C for 48 hours under continuous stirring. The white, semi-crystalline precipitate (**2a**) was filtered, washed with toluene, and dried in a desiccator under reduced pressure overnight (yield: 34.2 g, 54%). The intermediate **2a** (33.0 g, 146 mmol)

and Et_3N (24.3 g, 240 mmol) in CH_2Cl_2 (100 ml) were cooled to 0°C and a solution of methacryloyl chloride (18.8 g, 180 mmol) in CH_2Cl_2 (50 ml) was added dropwise over a period of 30 minutes. The reaction was stirred for 30 minutes at 0°C, then at ambient temperature for 18 hours. Following quantitative conversion of **2a** into **3a**, which was confirmed by ^{1}H NMR, the reaction was cooled to 0°C and the excess of methacryloyl chloride quenched with MeOH (20 ml). The product (**3a**) was then precipitated in ice-cold Et_2O for a minimum of 3 times. The residue was dissolved in dH_2O (300 ml) and transferred into a separation funnel. A solution of Na_2CO_3 (1.5×mol methacryloyl chloride, ~30 ml) was added to the separation funnel to deprotonate triethylamine hydrochloride and the aqueous layer was then washed with petroleum ether (2×200 ml) to remove any non-polar organic compounds. To exchange the counter ion, solid NaCl was added portion wise until saturation was reached (~60-100 g). The excess salt was filtered into a Buchner filter and the aqueous phase was then extracted with $CHCl_3$:2-propanol (3:1 vol/vol) for 4 times. The organic layers were combined, the solvent evaporated under reduced pressure, and residue purified by flash chromatography (EtOAc: MeOH gradient from 3:1 to 6:4 vol/vol). Following chromatography, the fractions containing the monomer (**3a**) were combined and the solvent removed under reduced pressure. The resulting residue was solubilised in THF and filtered to remove residual insoluble triethylammoniun hydrochloride which was still present in the product. The solvent was then removed under reduce to afford monomer (**3a**) as a white solid which was stored at 4°C (yield: 6.7 g, 21%).

2a: $C_8H_{20}BrNO$, FW: 226.15 g mol^{-1}; ^{1}H NMR (400 MHz, D_2O) δ_H 3.99 (t, *J*=5.2 Hz, 2H, HOCH_2), 3.44 – 3.34 (m, 8H, CH_2N$^+$(CH_2CH$_3$)$_3$), 1.29 (t, *J*=7.2 Hz, 9H, CH$_2$N$^+$(CH$_2$CH_3)$_3$). ^{13}C NMR (101 MHz, D_2O) δ_C 57.4, 54.8, 53.4, 6.8. Mass Spectrometry: expected m/z: 146.15 [M$^+$], found 146.06 [M$^+$]. FT-IR (neat): ν = 3216 (OH), 2981 (CH), 2944 (CH), 1628 (CC) cm^{-1}.

3a: $C_{12}H_{24}ClNO_2$, FW: 249.78 g mol^{-1}; ^1H NMR: δ_H (400 MHz, $CDCl_3$) 6.09 – 6.05 (m, 1H, CH), 5.64 – 5.60 (m, 1H, CH), 4.63 – 4.58 (m, 2H, $C(O)OCH_2$), 3.89 – 3.84 (m, 2H, OCH_2CH_2), 3.55 (q, J =7.3 Hz, 6H, ($^+N(CH_2CH_3)_3$), 1.91 – 1.87 (m, 3H, CH_3), 1.42 – 1.35 (m, 9H, ($^+N(CH_2CH_3)_3$). ^{13}C NMR: δ_C (101 MHz, $CDCl_3$) 166.3, 135.0, 127.3, 57.8, 55.8, 54.3, 18.3, 8.2. Mass Spectrometry: expected m/z: [M^+] 214, found 214 [M^+]. FT-IR (neat): ν= 2984 (CH), 2924 (CH), 1719 (CO), 1636 (CC) cm^{-1}.

Triethyl(2-(methacryloyloxy)ethyl)phosphonium chloride (3b): 2-Bromoethanol (13.8 g, 111 mmol) was dissolved in THF (100 ml) and the resulting solution was carefully deoxygenated by nitrogen bubbling for 30 min. A 1.0 M solution of Et_3P in THF (50 mL 5.9 g, 50 mmol) was then added under inert atmosphere (*CAUTION: Et_3P is spontaneously flammable in air, and must be handled under inert atmosphere*). The reaction mixture was stirred at 50°C for 48 hours. The reaction mixture was cooled down to room temperature, the supernatant was then decanted off and discarded, while the white precipitate at the bottom was re-solubilised in methanol (~30 ml) and precipitated in Et_2O (~600 ml). This procedure was repeated until a white solid product (**2b**) was obtained. The latter was filtered, washed with toluene and dried under reduced pressure overnight (yield: 17.5 g, 65%). The intermediate (**2b**) (17.5 g, 72 mmol) and Et_3N (14.6 g, 144 mmol) in CH_2Cl_2 (100 ml) were cooled to 0°C and a solution of methacryloyl chloride (11.3 g, 108 mmol) in CH_2Cl_2 (50 ml) was added dropwise. The reaction was stirred for 30 minutes on ice, followed by further 18 hours at ambient temperature. The reaction mixture was cooled to 0°C and the excess of methacryloyl chloride quenched with MeOH (50 ml). The final product (**3b**) was extracted using the same protocol described for monomer **3a**. The monomer was stored at 4°C (yield: 5.0 g, 26%).

2b: $C_8H_{20}BrPO$, FW: 243.12 g mol^{-1}; ^1H NMR: δ_H (400 MHz, $CDCl_3$) 4.15 (dt, *J* = 20.9, 5.8 Hz, 2H, $HOCH_2$), 2.68 (dt, *J* = 11.7, 5.8 Hz, 2H, $CH_2CH_2P^+$), 2.48 (dq, *J* = 13.0, 7.7 Hz, 6H, $CH_2P^+(CH_2CH_3)_3$), 1.35 (dt, *J* = 18.2, 7.7 Hz, 9H, $CH_2P^+(CH_2CH_3)_3$). ^{13}C NMR: δ_C (101 MHz, $CDCl_3$) 54.7 (d, *J* = 7.3 Hz), 21.9 (d, *J* = 49.3 Hz), 13.0 (d, *J* = 48.6 Hz), 6.0 (d, *J*=5.5 Hz). ^{31}P NMR: δ_P (162 MHz, $CDCl_3$) 38.85 ($^+P(CH_2CH_3)_3$). Mass Spectrometry: m/z: [M^+] 164.12 [M^+], found 164.01 [M^+]. FT- IR (neat): *v*= 3353 (OH), 2944 (CH), 2892 (CH), 1640 (CC) cm^{-1}.

3b: $C_{12}H_{24}ClO_2P$, FW: 266.74 g mol^{-1}; ^1H NMR: δ_H (400 MHz, $CDCl_3$) 6.12 – 6.08 (m, 1H, CH), 5.69 – 5.64 (m, 1H, CH), 4.57 (dt, *J* = 17.6, 6.3 Hz, 2H, $C(O)OCH_2$), 3.07 (dt, *J* =12.6, 6.3 Hz, 2H, OCH_2CH_2), 2.59 (dq, *J* = 13.0, 7.7 Hz, 6 H, ($^+P(CH_2CH_3)_3$), 1.93 (m, 3H, CH_3), 1.39 – 1.28 (m, 9H, ($^+P(CH_2CH_3)_3$). ^{13}C NMR: δ_C (101 MHz, $CDCl_3$) 166.4, 135.1, 127.2, 57.8 (d, *J* = 5.4 Hz), 19.1 (d, *J* = 48.4 Hz), 18.2, 13.1 (d, *J* =48.3 Hz), 6.2 (d, *J* = 5.5 Hz). ^{31}P NMR: δ_P (162 MHz, $CDCl_3$) 37.94 ($^+P(CH_2CH_3)_3$). Mass Spectrometry: m/z: [M^+] 231, found 231 [M^+]. FT- IR (neat): *v*= 2913 (CH), 2885 (CH), 1715 (CO), 1636 (CC) cm^{-1}.

***N,N,N*-triethyl-2-(2-(2-(methacryloyloxy)ethoxy)ethoxy)ethan-1-aminium chloride (3c):** Firstly, neat 2-[2-(2-chloroethoxy)ethoxy]ethanol (10 g, 59 mmol) was converted into its corresponding bromide by reaction with finely grounded NaBr (18.2 g, 177 mmol) at 70°C for 48 hours, under nitrogen atmosphere. The reaction was monitored by ^{13}C NMR following the reduction of the CH_2Cl signal at ~42 ppm and the appearance of a new signal at ~30 ppm for CH_2Br (**1c**). The conversion of 2-[2-(2-chloroethoxy)ethoxy]ethanol into its corresponding alkyl bromide was not quantitative (conversion was estimated to be ~57% as analyzed by ^{13}C NMR), however, this did not interfere with the following step, most likely because the bromide ions

generated *in situ* in that reaction could still facilitate the nucleophilic substitution with P or N nucleophiles to give the required ammonium and phosphonium salts. The product was resolubilised in CH_2Cl_2 (50 ml) and the excess of NaBr salt and formed NaCl were filtered off using a Buchner filter. CH_2Cl_2 was removed under reduced pressure and the resulting alcohol bromide intermediate was used for the following step without further purification. The intermediate **2c** and neat Et_3N were reacted at 75°C for 48 hours, under stirring. The brown bottom layer was separated from the yellow top phase, solubilised in MeOH, precipitated in Et_2O and utilized for the next step without further purification (yield: 11.6 g, 62% based on 2-[2-(2-chloroethoxy)ethoxy]ethanol utilized for the initial step). The crude intermediate (**2c**) (11.6 g, 37 mmol) was dissolved in CH_2Cl_2 (100 ml) and Et_3N (7.5 g, 74 mmol), and the resulting solution was cooled to 0°C. A solution of methacryloyl chloride (5.8 g, 56 mmol) in CH_2Cl_2 (50 ml) was added dropwise to the reaction and was stirred for 30 minutes on ice (0°C), then at ambient temperature for 18 hours. The completion of the reaction was confirmed by ^{1}H NMR and the excess of methacryloyl chloride was quenched in MeOH. The work up, including the conditions for flash chromatography on SiO_2, was carried out as described for (**3a**). The monomer was stored at 4°C (yield: 5.0 g, 40%).

2c: $C_{12}H_{28}BrNO_3$, FW: 314.26 g mol^{-1}; ^{1}H NMR: δ_H (400 MHz, $CDCl_3$) 4.02 (m, 2H, $OCH_2CH_2N^+$), 3.84 – 3.49 (m, 16H, $HOCH_2CH_2OCH_2CH_2OCH_2CH_2N^+(CH_2CH_3)_3$, 1.37 (t, J = 6.9 Hz, 9H, $N^+(CH_2CH_3)_3$). Mass Spectrometry: m/z: 234.21 [M^+], found 234.87 [M^+]. FT-IR (neat): ν= 3318 (OH), 2907 (CH), 2879 (CH), 1640 (CC), 1122 (CO) cm^{-1}.

3c: $C_{16}H_{32}ClNO_4$, FW: 337.88 g mol^{-1}; ^{1}H NMR: δ_H (400 MHz, $CDCl_3$) 6.00 (m, 1H, CH), 5.52 – 5.47 (m, 1H, CH), 4.20 – 4.14 (m, 2H, $C(O)OCH_2CH_2$), 3.87 (t, J = 9.0 Hz, 2H, $C(O)OCH_2CH_2$), 3.66 – 3.56 (m, 8H, $OCH_2CH_2OCH_2CH_2N^+$), 3.43 (q, J = 7.2 Hz, 6H, $N^+(CH_2CH_3)_3$), 1.85 – 1.82

(m, 3H, CH_3), 1.32 – 1.25 (m, 9 H, $N^+(CH_2C\mathit{H_3})_3$). ^{13}C NMR: δ_C (101 MHz, $CDCl_3$) 167.1, 135.9, 125.8, 70.5, 70.2, 69.0, 64.4, 63.6, 57.2, 54.3, 18.2, 8.22. Mass Spectrometry: m/z: [M^+] 302, found 302 [M^+]. FT-IR (neat): ν= 2980 (CH), 2943 (CH), 1713 (CO), 1635 (CC), 1124 (CO) cm^{-1}.

Triethyl(2-(2-(2-(methacryloyloxy)ethoxy)ethoxy)ethyl)phosphonium chloride (3d): Following the partial conversion of 2-[2-(2-chloroethoxy)ethoxy]ethanol (10 g, 59 mmol) into its corresponding bromide as described for monomer **3c**, the resulting intermediate was dissolved in THF (100 ml), the solution was carefully degassed by N_2 bubbling, and a 1.0 M solution of Et_3P in THF (47 mL, 5.5 g, 47 mmol) was added under inert atmosphere (*CAUTION: Et_3P is spontaneously flammable in air, and must be handled under inert atmosphere*). The reaction solution was then stirred at 50°C for 48 hours. After completion, two phases were observed. The desired phosphonium alcohol intermediate **2d** was found to be in the bottom phase of the reaction, as revealed by ^1H and ^{31}P NMR analysis. The top layer was then decanted off and the resulting brown residue was desiccated under reduced pressure (yield: 11.1 g, 59%). Next, the intermediate **2d** (11.1 g, 33.5 mmol), Et_3N (6.8 g, 67 mmol) were dissolved in CH_2Cl_2 (100 ml) and a solution of methacryloyl chloride (5.2 g, 50 mmol) in CH_2Cl_2 (50 ml) was added at 0°C over the duration of 30 minutes period, then stirred at ambient temperature for 18 hours. Completion of the reaction was confirmed by ^1H NMR and the excess of methacryloyl chloride was quenched with MeOH (30 ml) at 0°C. The crude residue was then purified as described for the other monomers. The monomer was stored at 4°C (yield: 7.67 g, 64%).

2d: $C_{12}H_{28}BrO_3P$, FW: 331.23 g mol^{-1}; ^1H NMR: (400 MHz, $CDCl_3$) δ_H 4.00 – 3.84 (m, 2H, $HOC\mathit{H_2}CH_2$), 3.78 – 3.49 (m, 10H, $HOCH_2C\mathit{H_2}OC\mathit{H_2}C\mathit{H_2}OC\mathit{H_2}C\mathit{H_2}P^+$), 2.55 – 2.39 (m, 6H, $^+P(C\mathit{H_2}CH_3)_3$, 1.29 (m, 9H, $^+P(CH_2C\mathit{H_3})_3$. ^{31}P NMR: (162 MHz, $CDCl_3$) δ_P 38.9 ($^+P(CH_2CH_3)_3$.

Mass Spectrometry: m/z: 251.33 [M^+], found 251.79 [M^+]. FT-IR (neat): *v*= 3433 (OH), 2980 (CH), 2960 (CH), 1635 (CC), 1124 (CO) cm^{-1}.

3d: $C_{16}H_{32}ClO_4P$, FW: 354.85 g mol^{-1}; ^1H NMR: δ_H (400 MHz, $CDCl_3$) 6.13 (m, 1H, CH), 5.66 – 5.61 (m, 1H, CH), 4.30 (t, *J* = 4.9 Hz, 2H, $C(O)OCH_2$), 3.94 (dt, *J* = 19.7, 5.9 Hz, 2H, $OCH_2CH_2P^+$), 3.77 – 3.61 (m, 6H, $C(O)OCH_2CH_2OCH_2CH_2OCH_2CH_2P^+$), 3.04 (dt, *J* = 12.2, 5.9 Hz, 2H, $OCH_2CH_2P^+$), 2.53 (dq, *J* = 13.5, 7.7 Hz, 6H, $^+P(CH_2CH_3)_3$), 1.96 (m, 3 H, CH_3), 1.31 (dt, *J* = 18.2, 7.7 Hz, 9H, $^+P(CH_2CH_3)_3$. ^{13}C NMR: δ_C (101 MHz, $CDCl_3$) 70.2 (s), 70.0 (s), 68.8 (s), 63.9 (d, *J* = 7.6 Hz), 63.5 (s), 19.7 (d, *J* = 49.7 Hz), 18.1 (s), 12.6 (d, *J* = 48.7 Hz), 5.8 (d, *J* = 5.5 Hz). ^{31}P NMR δ_P (162 MHz, $CDCl_3$) 38.75 ($^+P(CH_2CH_3)_3$). Mass Spectrometry: m/z: [M^+] 319, found 319 [M^+]. FT-IR (neat): *v*= 2940 (CH), 2888 (CH), 1715 (CO), 1637 (CC), 1112 (CO) cm^{-1}.

RAFT polymerization of methacrylate polymers (4a-d): General procedure: Monomer (**3a-d**), V-501 (initiator) and 4-cyano-4-(thiobenzoylthio)pentanoic acid (CTP, RAFT agent) were charged into a Schlenk tube along with D_2O:EtOH (3:1 vol/vol, 4 ml). The tube was sealed and degassed by four freeze-pump-thaw cycles. The reaction was started by immersing the Schlenk tube into an oil bath at 70°C. To monitor the reaction, samples were taken at various time-points for molecular weight and conversion analysis. The latter was monitored by ^1H NMR spectroscopy, following the decrease of the monomer vinyl signals (5.6 and 6.2 ppm) using the ester $C(O)OCH_2$ signal for monomer and polymer at ~ 4.5 ppm. Once the desired conversion was reached, the polymerization was stopped by placing the Schlenk tube in an ice bath and by exposing the reaction mixture to air. Polymers were precipitated in ice-cold THF and/or diethyl ether. The polymer CTA end-group was removed as described by Perrier and coworkers[45,46]. Briefly, the polymer was

dissolved in DMSO and AIBN was added (polymer: AIBN = 1:20 mol:mol). The reaction mixture was deoxygenated for 15 minutes by nitrogen bubbling and then reacted at 80°C for 3 hours. The polymers were then precipitated in THF, dried under reduced pressure and stored at 4°C.

Reaction conditions of RAFT polymerization: $[M]_0:[CTA]_0:[I]_0= 100:1:0.5$

Polymer **4a**: **3a** 1.0 g (4.0 mmol)**,** CTP 11 mg (0.040 mmol), V-501 6.5 mg (0.020 mmol);

Polymer **4b**: **3b** 1.0 g (3.75 mmol), CTP 10.4 mg (0.0370 mmol), V-501 6.1 mg (0.019 mmol);

Polymer **4c**: **3c** 1.0 g (2.9 mmol), CTP- 7.34 mg (0.0264 mmol), V-501-4.3 mg (0.013 mmol);

Polymer **4d**: **3d** 1.0 g (2.8 mmol), CTP- 7.8 mg (0.028 mmol), V-501- 4.5 mg (0.014 mmol);

4a: ^{1}H NMR: δ_H (400 MHz, D_2O) 4.39 (COOC*H*$_2$), 3.62 (OCH$_2$C*H*$_2$), 3.36 ($^+$N(C*H*$_2$CH$_3$)$_3$), 1.93 (CH$_2$ of polymer backbone), 1.29 ($^+$N(CH$_2$C*H*$_3$)$_3$), 1.18 – 0.78 (CH$_3$ of polymer backbone).

4b: ^{1}H NMR: δ_H (400 MHz, D_2O) 4.28 (COOCH$_2$), 2.68 (OCH$_2$C*H*$_2$), 2.25($^+$P(C*H*$_2$CH$_3$)$_3$), 2.04 – 1.58 (CH$_2$ of polymer backbone), 1.31 – 1.12 ($^+$P(CH$_2$C*H*$_3$)$_3$), 0.90 (CH$_3$ of polymer backbone).

4c: ^{1}H NMR: δ_H (400 MHz, D_2O) 4.11 (C(O)OCH$_2$), 3.86 - 3.67 (C*H*$_2$OC*H*$_2$C*H*$_2$OC*H*$_2$C*H*$_2$), 3.42 – 3.23 ($^+$N(C*H*$_2$CH$_3$)$_3$), 1.86 (CH$_2$ of polymer backbone), 1.24 (($^+$N(CH$_2$C*H*$_3$)$_3$), 0.92 (CH$_2$ of polymer backbone).

4d: ^{1}H NMR: δ_H (400 MHz, D_2O) 4.11 (C(O)OCH$_2$), 3.89 – 3.59 (C*H*$_2$OC*H*$_2$C*H*$_2$OC*H*$_2$), 2.51 (CH$_2$P$^+$), 2.22 ($^+$P(C*H*$_2$CH$_3$)$_3$), 1.84 (CH$_2$ of polymer backbone), 1.19 ($^+$P(CH$_2$C*H*$_3$)$_3$), 0.92 (CH$_3$ of polymer backbone).

Size exclusion chromatography (SEC): Size exclusion chromatography (SEC) was performed on a Polymer Labs GPC50 instrument fitted with a differential refractive index detector. Separations were performed on a pair of PLGel Mixed-D columns (300 × 7.5 mm) fitted with a matching guard column (50 × 7.5 mm). The mobile phase was 0.5% NH_4BF_4 (w/v) in *N,N*-

dimethylformamide at a flow rate of 1 ml min^{-1}. Poly(methyl methacrylate) narrow standards (2–800 kDa, Agilent/Polymer Labs) were used to calibrate the SEC, and sample molecular weights and polydispersity indices were calculated using Cirrus 3.0 Software (Polymer Labs).

Dynamic light scattering (DLS): DLS measurements were carried out using a Viscotek 802 DLS instrument (laser setting λ=830 ± 5 nm). Polymer stock solutions were prepared at 2.0 mg ml^{-1} in PBS and filtered using a Millex HA filter (Merck Millipore). Polyplexes were formed at N^+/P^- or P^+/P^- ratio 20 by mixing polymer and RNA (final concentration of RNA 0.02 µg $µl^{-1}$). Polyplexes were incubated for 30 minutes at room temperature and analyzed at 20°C. Each sample was run in triplicates with 10 runs of 10 seconds duration. Results were analyzed using an OmniSIZE software (Viscotek).

Zeta potential measurements: Zeta potential measurements were performed at N^+/P^- or P^+/P^- ratio 20 using a Malvern Zetasizer (scattering angle of 173°, 10 mW He-Ne laser), which was operated at a wavelength of 633 nm. Polymer stock solutions were prepared at 2.0 mg ml^{-1} in sterile, nuclease-free H_2O and filtered using a Millex HA filter. To obtain polyplexes at N^+/P^- or P^+/P^- ratio 20, the polymer was complexed with RNA and incubated for 30 minutes at room temperature (total volume 200 µl). Prior to zeta potential measurements nuclease-free water was added to each sample (800 µL) and injected into a zeta potential cuvette using a syringe. Zeta potential readings were performed at 25°C using a Malvern Zetasizer and data was acquired using the software (Malvern Zetasizer).

Gel retardation assay: Polyplexes were prepared at various N^+/P^- or P^+/P^- ratios (X = N or P; for 0.1:1; 0.5:1; 1:1; 2:1; 4:1; 5:1; 10:1). Polymer stock solutions (2.0 mg ml^{-1}) were prepared in PBS and filtered using a Millex HA filter. To form polyplexes equal volumes of RNA and polymer

were mixed, immediately vortexed for 30 seconds and incubated at room temperature for 30 minutes (total volume: 20 µl, containing 266 ng RNA and varying amounts of polymer according to the molar ratio). Prior to loading, 3 µl of loading buffer (30% vol/vol glycerol in RNAse free H_2O) was added to each sample and 20 µl of polyplex solution was loaded onto a 1.5 % w/vol TAE agarose gel, and run in 0.5× TAE buffer at 100V for 45 minutes. RNA was visualized with ethidium bromide under UV illumination using at 365 nm using a Fujifilm LAS-4000 imager. Gel images were processed using ImageJ (National Institutes of Health, http://imagej.nih.gov/ij/)[47,48].

Heparin displacement assay: siRNA polyplexes were prepared at N^+/P^- or P^+/P^- ratios of 20 as previously described for the gel retardation assay. After 30 minutes incubation at room temperature, increasing amounts of heparin (0-2 µg) in PBS (5 µl) were added to 20 µl polyplexes and the resulting solutions was incubated for 15 minutes at room temperature. Samples were mixed with 4 µl of loading buffer and a sample volume of 15 µl was immediately loaded on a 1.2% (w/vol) TAE agarose gel and run at 100V for 30 minutes. RNA was visualized with ethidium bromide under UV illumination at 365 nm using a Fujifilm LAS-4000 imager. Gel images were processed using ImageJ (National Institutes of Health, http://imagej.nih.gov/ij/)[47,48].

Cell culture and maintenance: Cell experiments were carried out with a stable transfected green fluorescent protein (GFP) expressing mouse 3T3 cell line and HeLa cells. For confocal imaging, a non-transfected 3T3 cell line was employed. Cells were maintained in Dulbecco's modified Eagle's medium (DMEM) supplemented with 2 mM L-glutamine, 1% penicillin/streptomycin and 10% foetal calf serum (FCS) under standard culture conditions (37°C, 5% CO_2). For cellular uptake and knockdown studies, cells were cultured in antibiotic-free medium (24 hours prior transfection and while performing the experiment) to minimize cell death and avoid any potential interaction with RNA-polyplexes. Cellular uptake studies were performed

in serum-free medium to avoid RNA degradation which may lead to false-positive signals caused by the fluorescent tag diffusing into the cell.

Cell viability (Resazurin assay): Cells were seeded in a 12 well plate at $5x10^4$ cells/well in complete growth medium. After 4 hours, polymer solutions (0-1.42 mM), relating to the cationic charge; prepared in complete DMEM growth media were added to the cells (1ml polymer solution per well). Cells were incubated with polymers for 48 hours followed by a Resazurin assay[49,50]. For the assay, the cell media was removed and cells were washed with PBS. A stock solution of Resazurin (diluted 1 in 10 in complete growth media) was added per well (1ml). Cells were incubated for 2 hours in the dark and 100 µl of cell supernatant was transferred into a 96-well plate to read the fluorescence at 540/590 nm (excitation/emission, Tecan plate reader Infinite 200). For data evaluation, the assay background containing media and Resazurin assay reagent were subtracted from all assay samples and the fluorescence readings of treated cells were normalized to untreated cells and expressed as percentage metabolic activity.

Resazurin assay reagent (stock solution): Resazurin sodium salt was made up to a concentration of 440 µM in phenol red-free HBSS with Ca^{2+} and Mg^{2+}. Aliquots were stored protected from light at -20°C.

Resazurin assay reagent (for cell viability assay): The Resazurin stock solution was diluted 1 in 10 in complete growth media and was added directly to the cells.

siRNA transfection (GFP): 3T3 cells were seeded in antibiotic-free medium in 12-well plates and grown overnight (~16-18 hours, cell confluence ~40%). For the preparation of polyplexes, siRNA was added to the appropriate polymer solution in PBS (100 µl) and the mixture was immediately vortexed (30 seconds) and incubated at room temperature for 30 minutes. In the

meantime, cell medium was replaced with 600 µl of serum free medium. Polyplexes were then added dropwise to the cells with gentle rocking. GFP knockdown was assessed by flow cytometry. Commercially available Interferin (Polyplus transfection) was employed as positive control following the manufacturer's recommendation.

Cellular uptake studies (confocal and flow cytometry): 3T3 cells were seeded in 12-well plates ($5x10^4$ cells/well) and were grown in antibiotic-free, complete growth medium overnight. For confocal imaging, cells were cultured on sterilized borosilicate cover slips in 12-well plates. Polymer-siRNA complexes (N^+/P^- or P^+/P^- 20:1) were prepared using Alexa Fluor 647 fluorescent labelled siRNA and added to the cells in serum free media (total volume 100 µl). The polyplex solutions were then added dropwise to 600 µl DMEM media in each well (final siRNA concentration 187 nM). Free, naked siRNA was included as control. Cells were incubated for 4 hours and relative cellular uptake was assessed by flow cytometry. Subcellular siRNA distribution was investigated by confocal microscopy.

Flow cytometry: 3T3 Cells were transfected with polyplexes (N^+/P^- or P^+/P^- ratio 20, 187 nM siRNA) in serum free medium and incubated in the dark for 4 hours. After incubation, cells were prepared and processed using FACS analysis (FC500, Beckman Coulter, Inc.). A minimum of 10,000 cells were analyzed for cellular uptake studies. Cell data was analyzed using the Flowing Software 2.5 (provided by Cell Imaging Core of the Turku Centre for Biotechnology). For data evaluation results were expressed as median fluorescence.

Confocal imaging: 3T3 cells were seeded onto sterilized borosilicate cover slips and were grown in antibiotic-free cell media. Polyplexes (N^+/P^- or P^+/P^- ratio 20, 187 nM) were prepared and added to the cells. After incubation (4 h), cells were gently washed in PBS (3×), fixed in 4%

paraformaldehyde solution for 10 minutes (room temperature), washed in PBS (3×) and stained using following staining procedures:

Wheat germ agglutinin, Alexa Fluor 488 (green): A 5 μg ml^{-1} working solution was prepared in HBSS and added to the cells (500 μl) and incubated for 10 minutes in the dark. Cells were washed in HBSS (3×) prior to further processing.

Hoechst nuclear counterstain: For nuclei counterstaining a 1 μg ml^{-1} Hoechst solution (33342, 1,4-diazabicyclo[2.2.2] octane) was prepared in HBSS and added to the cells (500 μl) for 7 minutes in the dark. Cells were washed in HBSS (3×) prior to further processing.

The cover slips were gently lifted out of the transwell plate and cells were mounted into 15 μl of glycerol solution on a glass slide. The edges of the cover slip were sealed with colourless nail vanish and dried for 5 minutes. Samples were stored in the dark at 4°C and analyzed within 3 days. Confocal imaging was performed using a confocal laser scanning microscope (Zeiss LSM510 Meta) equipped with a helium-neon (633 nm) and argon laser (488 nm). The nuclear dye (Hoechst) was excited using a mercury lamp. Images were taken at frame size 512 and scan average of 8. Z-stacks were collected at top and bottom of the cell borders at a size of 1 μm (stack interval) with a 512 frame size and scan average of 4. Images of at least two fields of view (10 or 40x magnification) were collected for every sample. Images were processed using LSM image browser (Zeiss) software and ImageJ (National Institutes of Health, http://imagej.nih.gov/ij/)[47,48].

Analysing GFP knockdown using flow cytometry: To analyze siRNA mediated knockdown, GFP-3T3 expressing cells were employed. Polyplexes containing siRNA targeting GFP were prepared at different N^+/P^- or P^+/P^- ratios and added to the cells in serum free media. After 4 hours, the medium was changed to antibiotic-free media and cells were incubated for a further 44 hours.

For analysis via flow cytometry, cells were washed in PBS (3×) and detached from the plate using 250 µl trypsin-EDTA for 5 minutes. Antibiotic-free DMEM media (1 ml) was added and cells were transferred in 1.5 ml Eppendorf tubes and centrifuged (250× g, 5 minutes). The cell pellet was resuspendend in ice-cold FACS buffer (500 µl, 2.5% FBS in 1× PBS) and spun (250× g, 5 minutes). Finally, the cell pellet was resuspended in 500 µl of FACS buffer and transferred into flow cytometry tubes. Cells (n >20,000) were analyzed using a FC 500 instrument (Beckman Coulter, Inc.) and Flowing Software 2.5 (Cell Imaging Core of the Turku Centre for Biotechnology). For data evaluation, the main cell population was gated to exclude cell debris within the side scatter/forward scatter dot plot and was further analyzed. Results were reported as median cell fluorescence intensity, normalized to the untreated cell population (cells only).

siRNA transfection (Survivin): HeLa cells were seeded in antibiotic-free medium in 12-well plates and were grown overnight (~16-18 hours). Polyplexes of siRNA/liRNA and polymer **4d** were prepared in PBS at different P^+/P^- ratio (100 µl) and added to were added dropwise into each well (final volume 1 ml). Cells were incubated for 24 hours and lysed in 500 µl Isol-RNA Lysis Reagent (5' Prime) and processed immediately or stored at -80°C (up to one week). Transfection experiments were performed with 30 nM of either siRNA or liRNA.

Isolation of RNA: To isolate RNA from total cell lysates, which were prepared by the addition of lysis buffer (Isol-RNA Lysis Reagent, 5' Prime), supernatants were transferred into 1.5 ml Eppendorf tubes and 100 µl chloroform was added to each sample. Samples were vortexed for 20 seconds and incubated at room temperature for 10 minutes. The supernatants were then centrifuged at 4°C for 25 minutes (16.1× g). The upper aqueous phase was transferred into a new tube and 180 µl isopropanol were added and samples were mixed for 5 seconds and incubated for further 10 minutes at room temperature. The tubes were then spun for 20 minute at 4°C (16.1× g). After

centrifugation the solution was carefully decanted off and 500 µl of ethanol (75 % vol/vol in RNAse free water) were added to the RNA pellet. The pellet was gently flicked and centrifuged for 10 minutes at maximum speed at 4°C. The ethanol supernatant was carefully decanted off and the pellet was air-dried and resuspended in 12 µl of RNAse-free water and solubilized by incubating it at 65°C for 3 minutes. The RNA concentration was determined by spectrophotometry using a Nanodrop spectrophotometer (BioSpec Nano, Shimadzu).

Production of cDNA templates for qRT-PCR analysis: RNA was transcribed into complementary DNA (cDNA) templates for further analysis using quantitative real-time PCR (qRT-PCR). cDNA synthesis was performed using a ImProm-II Reverse Transcription System (Promega) according to the manufacturer's protocol.

Quantitative reverse transcription real time polymerase chain reaction (qRT-PCR): Target gene levels (Survivin and GAPDH) were measured by qRT-PCR using a StepOne real time PCR system (Applied Biosystems) as described in the manufacturer's protocol. Samples were subjected to the following qRT-PCR programme: One cycle of 10 sec at 95°C, 40 cycles of 15 sec at 95°C, 20 sec at 60°C, 20 sec at 72°C followed by melt curve analysis. For quantification of gene expression, a relative quantification method was used to quantify Survivin mRNA levels relative to GAPDH expression.

RESULTS AND DICUSSION

This work focused on synthesizing a family of siRNA-binding polymers where both the nature of the permanently charged heteroatom and the length of the chemical spacer linking these cationic groups to the polymer backbone were systematically varied. Accordingly, polymers were prepared

with either ammonium or phosphonium quaternary salts, and oxyethylene or trioxyethylene spacers (Scheme 1). The first step of the synthesis of the required cationic monomers involved the conversion of an alkyl halide-alcohol into its corresponding ammonium or phosphonium salt by reaction with either triethylamine or triethylphosphine. The halides utilized were 2-bromoethanol and 2-[2-(2-bromoethoxy)ethoxy]ethanol leading to their corresponding ammonium or phosphonium salts (**2a-d**).

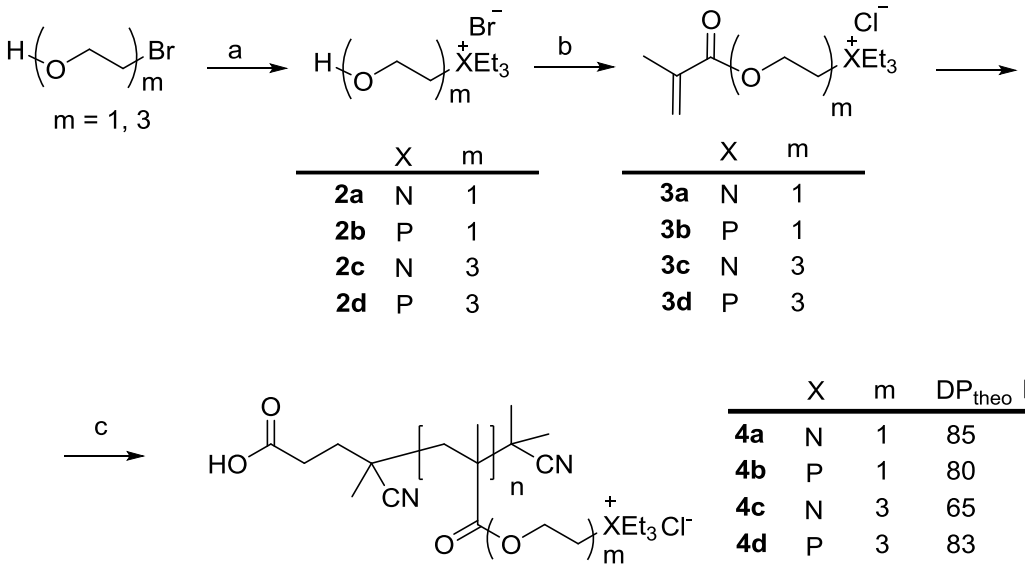

	X	m
2a	N	1
2b	P	1
2c	N	3
2d	P	3

	X	m
3a	N	1
3b	P	1
3c	N	3
3d	P	3

	X	m	DP_{theo}	$M_{n,SEC}$ (kDa)	PDi_{SEC}
4a	N	1	85	24.6	1.10
4b	P	1	80	18.1	1.10
4c	N	3	65	22.5	1.13
4d	P	3	83	27.5	1.15

Scheme 1. Synthesis of phosphonium- and ammonium-containing methacrylate (**3a-d**) monomers. *Reagents and conditions*: a. X=N: Et_3N, toluene, 75°C, 48 hours; X=P: 1.0 M Et_3P in THF, toluene, 50°C, 48 hours; b. *i.* methacryloyl chloride Et_3N, dichloromethane; *ii.* brine; c. *i.* V501, 4-cyano-4-thiobenzoylthio)pentanoic acid (CTB, CTA), EtOH:D_2O 3:1, 70°C. $[M]_0$:$[CTA]_0$:$[I]_0$= 100:1:0.5; *ii.* AIBN (20 eq.), DMSO, 80°C, 3 hours. DP_{theo} was calculated based on conversion at which the polymerization was stopped. M_n and PDi as measured by SEC in 0.5% NH_4BF_4 (w/v) in DMF as the mobile phase.

The alcohols (**2a-d**) were then treated with methacryloyl chloride and triethylamine in CH_2Cl_2 followed by counterion exchange with brine and flash chromatography, to give the required monomers (**3a-d**). The monomers were polymerized using aqueous RAFT polymerization giving a library with different length of the linker connecting the cationic moieties to the polymer backbone and nature of the heteroatom salts (ammonium or phosphonium).

Reversible Addition-Fragmentation chain Transfer (RAFT) polymerization of monomers (**4a-d**) was carried out using 4-cyano-4-thiobenzoylthio)pentanoic acid (CTB) as the chain transfer agent (CTA), V-501 as radical initiator using a molar ratio of $[M]_0$: $[CTA]_0$: $[I]_0$ = 100: 0.5: 1 in D_2O/EtOH (3:1 vol/vol) as solvent at 70°C. Deuterated solvent was used in the polymerization to facilitate monomer conversion monitoring by ^1H NMR. Polymerizations were controlled, as demonstrated by substantially linear first-order kinetics. In some cases an initial induction time, typical of RAFT polymerization[51,52] was observed (see supporting information). The polymers were precipitated in Et_2O or THF to remove unreacted monomers and low molecular weight impurities. Then, the dithioester CTA moieties at the end of the polymer chains were removed following the Perrier method[53]. All polymers were found to be water-soluble, with low polydispersity indices (PDi_{SEC}: 1.10-1.15).

siRNA complexation studies. The ability of polymers (**4a-d**) to bind siRNA was first assessed in a gel retardation assay to estimate the amount of polymer required to quantitatively bind RNA. Polymers were complexed with siRNA at different N^+/P^- or P^+/P^- ratios (0.1, 0.5, 1, 2, 4, 5, 10) - the molar ratio between the positively charged polymer repeating units, and the anionic phosphate groups on siRNA After incubation of 30 minutes at room temperature, products were analysed by agarose gel electrophoresis. All polymers were found to quantitatively bind siRNA at N^+/P^- or P^+/P^- ratio between 1 and 2 (2 being the first ratio where no free siRNA was detected) (Figure 1A).

Semi-quantitative analysis was carried out by fitting the data to a modified Hill's equation, which suggested that phosphonium-based polymers bound siRNA slightly better than corresponding ammonium analogues (K_{4a} = 0.62 ± 0.04 vs. K_{4b} =0.43 ± 0.05) for polymers with shorter linker and longer linker (K_{4c} =0.39 ± 0.08 and K_{4d} =0.28 ± 0.06) (Figure 1B, Table 1). K values reflect the amount of polymer required to complex 50% of the siRNA in the incubation samples, thus the polymers with better ability to complex siRNA possess the lowest K. Furthermore, the length of the oxyethylene linker seemed to influence polymer binding, with better binding observed for polymers containing the longer linker (**4a** *vs.* **4c**, and **4b** *vs.* **4d**). These results are in agreement with previous reports which demonstrated better binding for phosphonium based polymers over their corresponding ammonium analogues, [38,39] although for the systems investigated in this present work the observed difference was relatively modest.

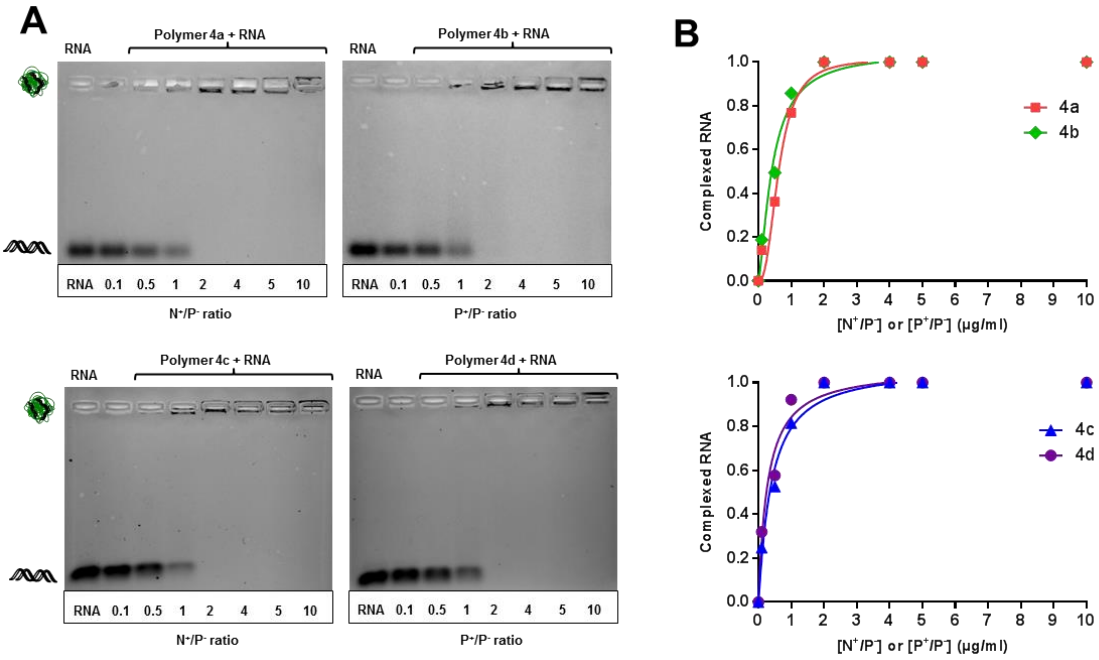

Figure 1: A) Gel retardation assay with siRNA and polymers (**4a-d**). Polyplexes were formed at different N^+/P^- or P^+/P^- ratios. Samples were incubated for 30 minutes at room temperature before loading onto a 1.5% w/vol agarose gel (100V, 45 minutes). Representative gel images are shown, from three independent experiments. B) Estimation of polymer/RNA binding by fitting data into a modified Hill's equation. Data was plotted as complexed RNA at different polymer concentrations (μg/ml), expressed here as N^+/P^- or P^+/P^- ratio.

Table 1: Hill's equation's binding constant K, representing half-maximum binding at 30 minutes for siRNA polyplexes. K is expressed as polymer concentration (μg/ml) N^+/P^- or P^+/P^- ratio. Data represents best-fit values ± SD.

Polymer	Atom	K (μg/ml)	K (N^+/P^- or P^+/P^- ratio)
4a	N	12.8 ± 0.8	0.62 ± 0.04
4b	P	9.4 ± 1.2	0.43 ± 0.05
4c	N	10.8 ± 2.2	0.39 ± 0.08
4d	P	8.2 ± 1.6	0.28 ± 0.06

The ability of polymers to retain siRNA upon complex formation in the presence of competitive polyanionic ligands was analyzed in a heparin displacement assay. Polyplexes were formed at N^+/P^- or P^+/P^- ratio of 20 and increasing amounts of heparin sodium salt were added and the incubation mixtures analyzed by agarose gel electrophoresis (Figure 2). For polymers with the short oxyethylene spacer (**4a**, **4b**), RNA displacement occurred following addition of 0.7-1.0 μg heparin with the ammonium polymer **4a** showing a slightly better tendency to bind RNA than its phosphonium analogue **4b**. In contrast, complexes formed with polymers with the longer

trioxyethylene linker, **4c** and **4d,** were more stable, with RNA displaced by the addition of 1.0-1.3 and 1.3-1.7 µg heparin, respectively. These results indicate that polyplexes formed with polymers with the longer linker had higher stability in the presence of heparin than their corresponding analogues. In addition, polyplexes formed with phosphonium polymer **4d** were found to be more stable under these conditions than its ammonium analogue **4c** suggesting an effect of the nature of the charged heteroatom on the stability of the resulting polycomplex. This behaviour could be ascribed to a different charge distribution within the alkylphosphonium cation, together with larger cationic size which potentially favours nucleic acid binding with phosphonium-based polymers as the positive charge is more localised on the heteroatom and less diffused in comparison to ammonium based polymers[38,39]. In addition, the binding and stability results indicate that polymers with longer trioxyethylene linker have improved binding with nucleic acids, possibly due to enhanced macromolecular flexibility which allow them to rearrange their chain conformation around the RNA molecules, achieving more efficient binding.

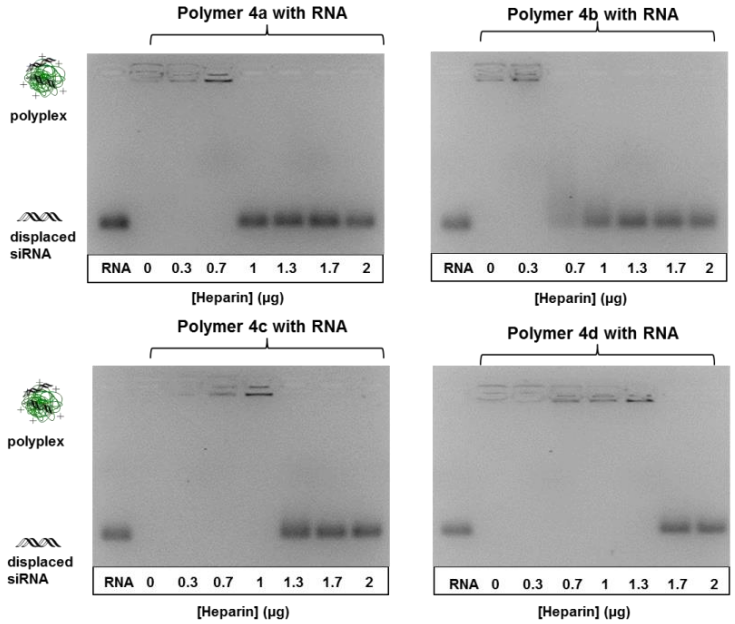

Figure 2: Heparin displacement assay. Polyplexes of N^+/P^- or P^+/P^- 20 were prepared and incubated for 30 minutes at room temperature. Increasing concentrations of heparin were added and samples were incubated for 15 minutes prior to analysis by 1.2% agarose gel electrophoresis (100V, 30 minutes). A representative image of each experiment is shown.

Efficient cell uptake of polyplexes is highly dependent on their size and net charge. For DLS and zeta potential studies N^+/P^- or P^+/P^- ratios of 20 were chosen, as preliminary experiments using agarose gel electrophoresis confirmed efficient binding of nucleic acid under these conditions. This would also likely result in a proportion of unbound polymer chains in the polyplex formulations, which in some cases has been shown to be beneficial for improved gene knockdown and/or transfection *in vitro*[54,55]. While DLS measurements can be presented as intensity distribution results may be misleading, when studying a heterogeneous sample population, in which larger particles can dominate the sample due to an increase in light scattering[56,57]. To give an overview of the actual mass distribution with the sample population, the intensity distribution can be converted into mass by employing a mathematical model using the Mie theory[56,57]. While polymers (**4a-d**), RNA polyplexes ranged from ~ 4-15 nm in radius with polymer **4d** forming the smallest RNA polyplex (~4 nm) and polymer **4c** the largest (~15 nm). For RNA polyplexes formed with polymers **4a-c**, traces corresponding to larger aggregates were also detected (Figure 3 and Supplementary data). The zeta potential at N^+/P^- or P^+/P^- ratios 20 in aqueous medium showed a net positive surface charge for all polyplexes (~ +24-31 mV).

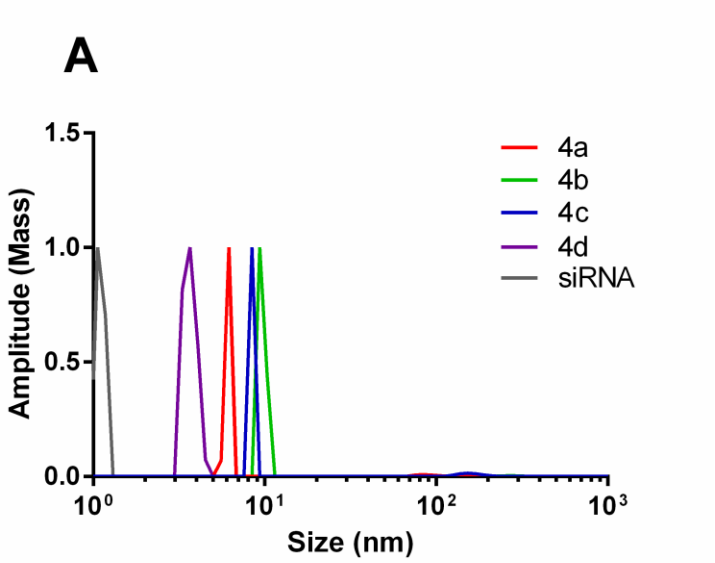

Polyplexes	R_h (nm)	Zeta- potential (mV)
siRNA	1.02 ± 0.07	−21.9 ± 5.3
4a	8.8 ± 2.2	30.1 ± 6.9
4b	13.7 ± 5.6	24 ± 2.8
4c	14.8 ± 6.9	30.5 ± 3.7
4d	4 ± 1	31.3 ± 3.4

Figure 3: Dynamic light scattering and zeta potential measurement of RNA polyplexes at N^+/P^- or P^+/P^- ratio 20. A) For DLS measurements polyplexes were prepared in PBS using a final concentration of 0.02 µg $µl^{-1}$ RNA in each sample. The table gives an overview of results for DLS and zeta potential measurements for RNA polyplexes (main population) at N^+/P^- or P^+/P^- ratio of 20.

The effect of polymers (**4a-d**) on the cell viability was evaluated using a Resazurin metabolic cell assay[49] (Figure 4). Metabolically active and hence viable cells convert Resazurin substrate into fluorescent Resorfurin, the amount of which is directly proportional to the cell number of viable cells (provided they are within the linear range of the detection)[50]. Fibroblast 3T3 cells were exposed to increasing polymer concentrations (0-1.4 mM of cationic repeating units) for 48 hours. The results indicated good cell viabilities (≥75%) for all polymers up to concentrations of 0.42 mM (which is above the polymer concentration utilized in subsequent cell studies), whilst a reduction of metabolic activity was found when using concentrations ≥ 0.56 mM (**4a-d**) which corresponds to 140-200 µg ml^{-1}, depending on the polymer investigated. In contrast, PEI (branched, 25kDa), a polymer commonly utilized for DNA/RNA complexation, showed a high cytotoxicity at all concentrations (6-60 µg ml^{-1}) investigated.

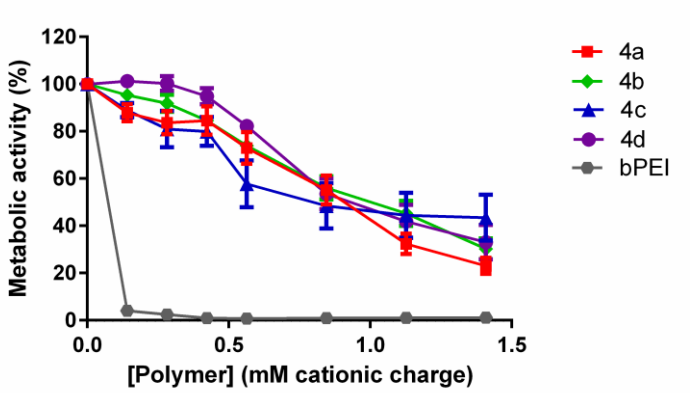

Figure 4: Cell viability assay following polymer exposure. Cells (mouse 3T3) were exposed increasing polymer concentrations. Cell viability was assessed using a resazurin assay after 48 hours exposure. Branched poly(ethylene imine) (25 kDa, bPEI) was used as a control. Error bars indicate the standard error of the mean (n=3).

Poly(meth)acrylates have been widely investigated for biomedical applications[58,59]. Clinically they are routinely utilized as biocompatible and biodurable materials in a range of applications which include intraocular lenses[60], orthopedic implant fixation[61], dentistry[62], and the manufactory of drug-eluting coronary stents[63]. This part of the present study suggests that these phosphonium-based materials are not cytotoxic at concentrations suitable for RNAi in vitro, although further in vivo studies will be needed to investigate their pharmacokinetic profiles and long-term biocompatibility.

The ability of polyplexes to mediate RNA uptake by 3T3 cells was investigated by flow cytometry and confocal microscopy. Polyplexes were formed with Alexa Fluor 647-conjugated siRNA (187 nM final concentration per sample) at N^+/P^- or P^+/P^- ratios of 20, and incubated with the cells for 4 hours. In flow cytometry measurements a strong increase of fluorescence was observed for all polyplexes in comparison to naked RNA (Figure 5A/B). Higher fluorescence was observed for polymers with the shorter linker (**4a-b**) in comparison to polymers with the longer trioxyethylene spacer. To investigate whether the observed fluorescence resulted from cell surface-bound fluorescent species or cellular uptake of polyplexes, confocal imaging was performed (Figure 5 C/D). Quantitative analysis of confocal images confirmed the internalization of polyplexes (≥75%).

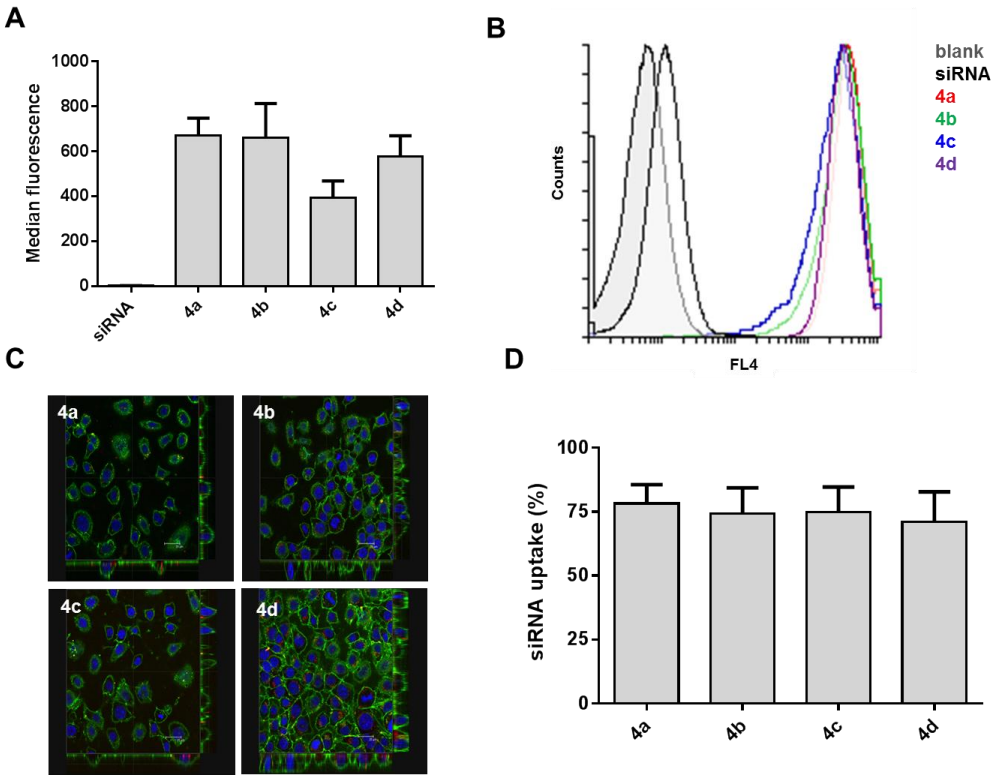

Figure 5: Cellular uptake of Alexa Fluor 647-conjugated RNA polyplexes (**4a-d**) by 3T3 cells: flow cytometry (A/B) and confocal imaging (C/D). A) For flow cytometry 2×10^4 3T3-GFP cells were analyzed, and results were normalized to the median fluorescence intensity of untreated cells. Data is represented as median fluorescence, error bars indicate the standard error of the mean (n=3). B) Representative histogram overlays of RNA (negative control) and polyplexes (**4a-d**) C) For confocal laser scanning microscopy 3T3 cells were cultured on borosilicate glass slides (12-well plates) and uptake was analyzed after 4 hours exposure. Cellular uptake of RNA-polyplexes can be observed by the internalization of RNA (red fluorescence) within in the cell. Cell plasma membrane is stained in green and the cell nucleus stained in blue. Representative images shown, scale bar: 25 µm D) Quantitative analysis of siRNA uptake (%) as analyzed by confocal imaging. A minimum of three representative images containing 45-60 cells in total) of three different

experiments were analyzed. SiRNA uptake represents the percentage of cells with internalized siRNA. Error bars indicate the standard error of the mean (n=3).

Whilst flow cytometry and confocal microscopy showed good cellular uptake for all polyplexes, all polymers (**4a-d**) investigated failed to mediate siRNA knockdown when targeting GFP in GFP-expressing 3T3 cells as analyzed flow cytometry. In contrast, commercially available Interferin successfully reduced GFP fluorescence by 71% in comparison to untreated cells (see supplementary data). Polyplexes were incubated for 48 hours at N^+/P^- or P^+/P^- ratio 5 or 20 using 187 nM total siRNA per sample. Recent studies by Reineke[54] and Yue[55] suggested that an excess of polymer within a polymer formulation increases cellular knockdown. For both N^+/P^- or $P^{+/}P^-$ ratios (5 and 20) investigated here, good RNA binding was achieved as demonstrated by a gel retardation assay (Figure 1). In parallel to knockdown experiments, cell viability studies were performed to evaluate if the RNA polyplexes (at a N^+/P^- or $P^{+/}P^-$ ratio 20 and/or 5) display cellular toxicity when incubated with cells *in vitro* (48 hours). The results indicated that treatment with RNA formulations at experimental conditions employed for transfection experiments did not affect cell metabolic activity, highlighting the non-toxic nature of polymers and deriving polyplex formulations, under the range of concentrations investigated (see supplementary data).

Taken together these experiments showed that although polymers (**4a-d**) mediated efficient RNA uptake in 3T3 cells while being non-toxic, they were unable to promote detectable levels of mRNA knockdown. One possible explanation is that their RNA polyplexes may not undergo efficient endosomal escape, and eventually be degraded in lysosomes. This could be ascribed to the polymers possessing permanently charged moieties unable to promote endosomal escape routes like "proton sponge" effects[64]. However, gene knockdown mediated by permanently

charged polymers with no endosomolytic moieties has been reported[38,65,66], which prompted us to further vary additional structural parameters in the polyplexes – i.e. the macromolecular architecture of the RNA payload - and investigate its effect of gene knockdown efficiency.

Effect of RNA molecular architecture on gene knockdown. Recently, multimeric RNAs with well-defined macromolecular architectures - tripodal, cross-shaped, and linear long interfering siRNA – have emerged as efficient tools to enhance gene delivery and knockdown efficiency[67,68]. These novel RNA multimers were found to particularly efficient in mediating RNAi, due to both enhanced ability to complex various cationic non-viral delivery vectors, and increased RNA cell uptake, compared to relatively small and stiff siRNA. In a recent study by Sajeesh et al. long interfering RNA has been used to form nanocomplexes with cationic polymer systems such as branched PEI (25 kDa) and linear PEI (25 kDa)[69]. Improved ability to form polyplexes at lower N^+/P^- ratio was observed for liRNA formulations compared to those where "conventional" shorter siRNA was employed as analyzed by DLS and AFM. Polyplexes with liRNA were also found to be more stable in the presence of competitive polyanionic ligands, as revealed by heparin displacement assay. A reduction of Survivin mRNA expression to ~20% using branched PEI at N^+/P^- ratio of 5 with 30 nM liRNA was achieved, as revealed by qRT-PCR analysis. In contrast, no knockdown was achieved using various PEI-siRNA under otherwise identical experimental conditions. In this present work we aimed at investigating the effect of RNA architecture on gene knockdown, utilising one of our phosphonium polymethacrylates polymers. For this part of our study, polymer **4d** was selected to generate polyplexes with liRNA targeting Survivin. To generate liRNA, the RNA sequence was designed in a way that annealing of complementary sense and

antisense strands leads to a long overhang which enables the addition of a further RNA strand creating a new long overhang (Figure 6A).

Pleasingly, **4d**-liRNA polyplexes mediated efficient mRNA knockdown of Survivin in HeLa cells (~65 %) when employing a P^+/P^- ratio of 10, using 30 nM liRNA (Figure 6B). Interestingly, lower knockdown of Survivin was observed when using a higher P^+/P^- ratio of 20, confirming that the engineering of the formulation for a given polymer/RNA system is an important parameter which should be considered in formulation design. In contrast, no significant knockdown was observed for shorter conventional siRNA targeting Survivin expression, revealing that for this specific polycationic polymer/RNA system, multimeric siRNAs was a superior agents for RNAi. (Please note that successful knockdown of Survivin using siSurvivn and commercially transfection agents was previously demonstrated[69–71]). The effect of polymer (**4d**) on the cell viability was assessed using a Resazurin metabolic cell assay[49] (Figure 6C). HeLa cells were exposed to increasing polymer concentrations (0-1.4 mM of cationic repeating units) for 48 hours. In agreement with results obtained using mouse 3T3 cells (Figure 4), the results indicated good cell viabilities (≥75%) up to concentrations of 0.56 mM and above, making polymer **4d** a suitable delivery vectors for cellular *in vitro* studies.

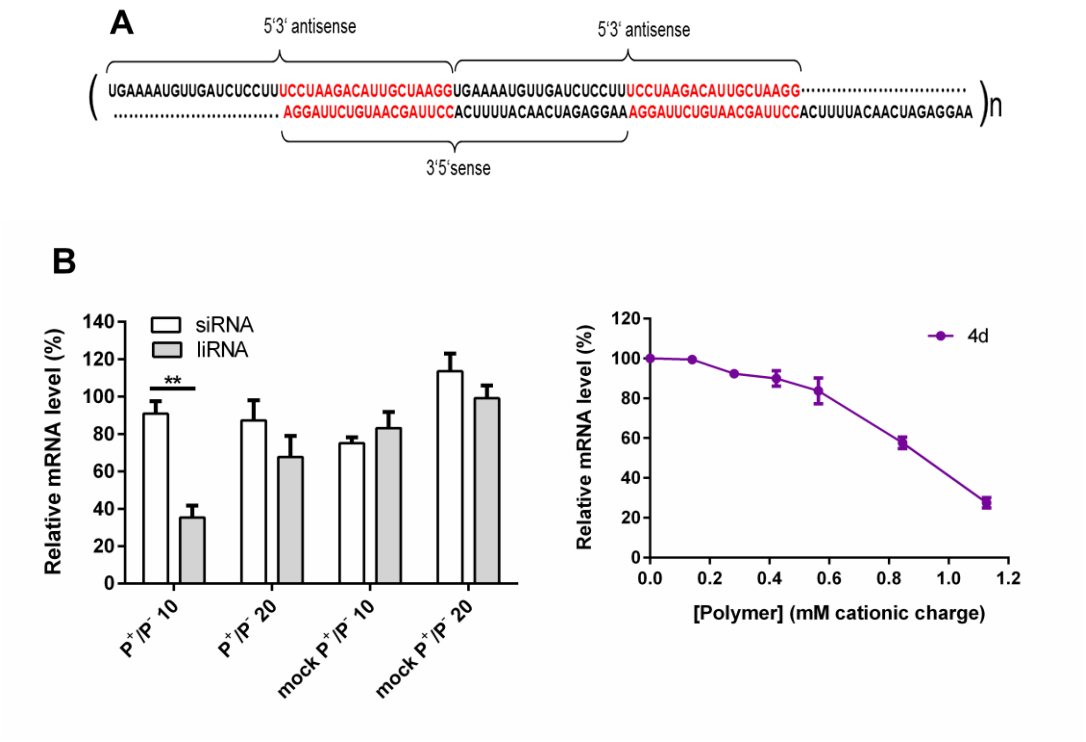

.

Figure 6: A) Structure of liRNA targeting Survivin. Please note that the last 19 nucleotides of the 5'3 antisense strand (red) are complementary to the first 19 nucleotides of the 3'5 sense strand (red). In addition, the first 19 nucleotides of the 5'3 antisense strand (black) are complementary to the last 19 nucleotides of the 3'5 sense strand (black). The specific RNA design enables multimerization due to a long overhang which enables the addition of a further RNA strand creating a new overhang. B) Knockdown studies with siRNA and liRNA targeting Survivin. HeLa cells were transfected with polymer **4d** using a P^+/P^- ratio of 10 and 20, with 30 nM siRNA or liRNA targeting Survivin. Survivin and GAPDH mRNA levels were measured by qRT-PCR 24 hours after transfection. Relative mRNA levels were determined by comparison of cells treated with siRNA/liRNA targeting Survivin and non-targeting control siRNA/liRNA. Data is represented as relative mRNA level (%) mean ± SEM and was analyzed by one-way ANOVA

followed by Turkey's multiple comparison, (**p ≤ 0.01) C) Resazurin cell viability assay for polymer **4d** in HeLa cells (n=3).

CONCLUSIONS

In this work we present an efficient route for the synthesis of phosphonium-containing polymers, an emerging class of materials for nucleic acid binding and delivery. By using aqueous RAFT polymerization, a family of well-defined cationic polymethacrylates with with low polydispersity (PDi_{SEC} = 1.1-1.15) were prepared. Both the nature of the charged heteroatom – P vs. N – and length of the spacer connecting the cationic moieties to the polymer backbone –oxyethylene vs. trioxyethylene– were systematically varied. Both parameters were found to affect the ability of polymers to bind siRNA. Phosphonium-based polymers showed marginally better siRNA binding (at lower P^+/P^- ratio) than their corresponding ammonium analogues as estimated by Hill's analysis. In addition, polymers with a longer trioxyethylene spacer between the charged heteroatoms and the polymer backbone showed better siRNA binding than those containing a shorter oxyethylene linker, possibly due to increased polymer flexibility, which would allow a more efficient rearrangement of the cationic repeating units to bind the phosphate groups of the relatively rigid rod-like siRNA molecules.

Although RNA polyplexes with polymers (**4a-d**) were all efficiently internalized by GFP-expressing 3T3 cells, no detectable siRNA-mediated GFP knockdown was observed. While further work will be needed to better understand this phenomenon, one likely explanation could be poor polyplex endosomolytic escape, although other experimental design factors, such as the choice of cell line and experimental conditions chosen for the knockdown studies may also play an important role.

By contrast, using phosphonium polymer **4d**, efficient Survivin mRNA knockdown was observed in HeLa cells when siRNA was replaced with multimerised liRNA demonstrating a strong effect of RNA structure on the efficiency of RNA interference. Future work will focus on how additional macromolecular features of both polymer – chain length and macromolecular architecture (e. g. linear vs. star), and RNA - RNA multimers such as liRNA, tripodal and quadruple interfering RNA[69,72,73] – affect intracellular trafficking and mRNA knockdown.

ASSOCIATED CONTENT

Supporting Information: Figure S1: Kinetic plots for the RAFT polymerization, Figure S2: Illustrations of modified Hill's equation, S3: Results of DLS and zeta potential measurements for RNA polyplexes, Figure S4: Cellular uptake by flow cytometry, additional data, S5: Knockdown studies, S6: Cell viability after polymer exposure, S7: Knockdown studies.

AUTHOR INFORMATION

Corresponding Author: giuseppe.mantovani@nottingham.ac.uk

Author contributions: The manuscript was written through contributions of all authors. All authors have given approval to the final version of the manuscript.

ACKNOWLEDGMENT

The project has been funded by AstraZeneca and the Engineering and Physical Sciences Research Council (EPSRC) through the EPSRC/AstraZeneca Centre for Doctorial Training (CDT) in Targeted Therapeutics and Formulation Sciences (EP/D501849/1) as well as through funding received by EP/J02158X/1. Further support from Global Research Laboratory grant (2008-00582) and National Research Foundation-Korea [NRF-2013R1A1A2064660] programme is also acknowledged.

REFERENCES

(1) Haussecker, D., and Kay, M. A. (2015) Drugging RNAi. *Science (80-.). 347*, 1069–70.

(2) Crunkhorn, S. (2013) Trial watch: Success in amyloidosis trials supports potential of systemic RNAi. *Nat. Rev. Drug Discov. 12*, 818.

(3) Wu, S. Y., Lopez-Berestein, G., Calin, G. A., and Sood, A. K. (2012) Targeting the undruggable: Advances and obstacles in current RNAi therapy. *Sci Transl Med. 6*, 240ps7.

(4) Spagnou, S., Miller, A. D., and Keller, M. (2004) Lipidic carriers of siRNA: differences in the formulation, cellular uptake, and delivery with plasmid DNA. *Biochemistry 43*, 13348–56.

(5) Shim, G., Kim, M.-G., Park, J. Y., and Oh, Y.-K. (2013) Application of cationic liposomes for delivery of nucleic acids. *Asian J. Pharm. Sci. 8*, 72–80.

(6) Xu, L., and Anchordoquy, T. (2011) Drug Delivery Trends in Clinical Trials and Translations Medicine: Challenges and Opportunities in the Delivery of Nucleic Acid-Based Therapeutics. *J Pharm Sci. 100*, 38–52.

(7) Han, H. D., Mangala, L. S., Lee, J. W., Shahzad, M. M. K., Kim, H. S., Shen, D., Nam, E. J., Mora, E. M., Stone, R. L., Lu, C., Lee, S. J., Roh, J. W., Nick, A. M., Lopez-Berestein, G., and Sood, A. K. (2010) Targeted gene silencing using RGD-labeled chitosan nanoparticles. *Clin. Cancer Res. 16*, 3910–22.

(8) Silva, A. T., Nguyen, A., Ye, C., Verchot, J., and Moon, J. H. (2010) Conjugated polymer nanoparticles for effective siRNA delivery to tobacco BY-2 protoplasts. *BMC Plant Biol. 10*, 291.

(9) Siegwart, D. J., Whitehead, K. A., Nuhn, L., Sahay, G., Cheng, H., Jiang, S., and Ma, M. (2011) Combinatorial synthesis of chemically diverse core-shell nanoparticles for intracellular delivery. *PNAS 108*, 12996–3001.

(10) Coburn, G. A., and Cullen, B. R. (2003) siRNAs: a new wave of RNA-based therapeutics. *J. Antimicrob. Chemother. 51*, 753–6.

(11) Duncan, R. (2011) Polymer therapeutics as nanomedicines: new perspectives. *Curr. Opin. Biotechnol. 22*, 492–501.

(12) Troiber, C., and Wagner, E. (2011) Nucleic acid carriers based on precise polymer conjugates. *Bioconjug. Chem. 22*, 1737–52.

(13) Son, S., Namgung, R., Kim, J., Singha, K., and Kim, W. J. (2012) Bioreducible polymers for gene silencing and delivery. *Acc. Chem. Res. 45*, 1100–12.

(14) Benoit, D. S. W., Srinivasan, S., Shubin, A. D., and Stayton, P. S. (2011) Synthesis of folate-functionalized RAFT polymers for targeted siRNA delivery. *Biomacromolecules 12*, 2708–2714.

(15) Jensen, S. A., Day, E. S., Ko, C. H., Hurley, L. A., Janina, P., Kouri, F. M., Merkel, T. J., Luthi, A. J., Patel, P. C., Cutler, J. I., Daniel, W. L., Scott, A. W., Rotz, M. W., Meade, J., Giljohann, D. A., Mirkin, C. A., and Stegh, A. H. (2014) Spherical Nucleic Acid Nanoparticle Conjugates as an RNAi-Based Therapy for Glioblastoma. *Sci Transl Med. 5*, 209ra152.

(16) Kim, H. J., Takemoto, H., Yi, Y., Zheng, M., Maeda, Y., Chaya, H., Hayashi, K., Mi, P., Pittella, F., Christie, R. J., Toh, K., Matsumoto, Y., Nishiyama, N., Miyata, K., and Kataoka, K. (2014) Precise Engineering of siRNA Delivery Vehicles to Tumors Using Polyion Complexes and Gold Nanoparticles. *ACS Nano 8*, 8979–8991.

(17) Ding, Y., Jiang, Z., Saha, K., Kim, C. S., Kim, S. T., Landis, R. F., and Rotello, V. M. (2014) Gold nanoparticles for nucleic acid delivery. *Mol. Ther. 22*, 1075–83.

(18) Lytton-Jean, A. K. R., Langer, R., and Anderson, D. G. (2011) Five years of siRNA delivery: Spotlight on gold nanoparticles. *Small 7*, 1932–1937.

(19) Forrest, M. L., Gabrielson, N., and Pack, D. W. (2005) Cyclodextrin-polyethylenimine conjugates for targeted in vitro gene delivery. *Biotechnol. Bioeng. 89*, 416–23.

(20) Lutz JF, Ouchi M, Liu DR, S. M. (2013) Sequence-Controlled Polymers. *Science (80-.). 341*, 1238149.

(21) Zhang, Q., Collins, J., Anastasaki, A., Wallis, R., Mitchell, D. A., Becer, C. R., and Haddleton, D. M. (2013) Sequence-controlled multi-block glycopolymers to inhibit DC-SIGN-gp120 binding. *Angew. Chemie - Int. Ed. 52*, 4435–4439.

(22) Matyjaszewski, K., and Tsarevsky, N. V. (2014) Macromolecular engineering by atom transfer radical polymerization. *J. Am. Chem. Soc. 136*, 6513–6533.

(23) Moad, G. (2015) RAFT Polymerization – Then and Now. *ACS Symp. Ser.*, pp 211–246.

(24) Gody, G., Maschmeyer, T., Zetterlund, P. B., and Perrier, S. (2013) Rapid and quantitative one-pot synthesis of sequence-controlled polymers by radical polymerization. *Nat. Commun. 4*, 2505.

(25) Zhang, Q., Wilson, P., Li, Z., Mchale, R., Godfrey, J., Anastasaki, A., Waldron, C., and Haddleton, D. M. (2013) Aqueous Copper-Mediated Living Polymerization: Exploiting Rapid Disproportionation of CuBr with Me6TREN. *J. Am. Chem. Soc. 135*, 7355–7693.

(26) Anastasaki, A., Nikolaou, V., Zhang, Q., Burns, J., Samanta, S. R., Waldron, C., Haddleton, A. J., McHale, R., Fox, D., Percec, V., Wilson, P., and Haddleton, D. M. (2014) Copper(II)/tertiary amine synergy in photoinduced living radical polymerization: Accelerated synthesis of ω-functional and α,ω-heterofunctional poly(acrylates). *J. Am. Chem. Soc. 136*, 1141–1149.

(27) York, A. W., Zhang, Y., Holley, A. C., Guo, Y., Huang, F., and McCormick, C. L. (2009) Facile Synthesis of Multivalent Folate-Block Copolymer Conjugates via Aqueous RAFT Polymerization: Targeted Delivery of siRNA and Subsequent Gene Suppression. *Biomacromolecules 10*, 936–943.

(28) Cho, H. Y., Srinivasan, A., Hong, J., Hsu, E., Liu, S., Shrivats, A., Kwak, D., Bohaty, A. K., Paik, H.-J., Hollinger, J. O., and Matyjaszewski, K. (2011) Synthesis of Biocompatible PEG-Based Star Polymers with Cationic and Degradable Core for siRNA Delivery. *Biomacromolecules 12*, 3478–86.

(29) Boyer, C., Bulmus, V., Davis, T. P., Ladmiral, V., Liu, J., and Perrier, S. (2009) Bioapplications of RAFT polymerization. *Chem Rev. 109*, 5402–5436.

(30) Heredia, K. L., Nguyen, T. H., Chang, C.-W., Bulmus, V., Davis, T. P., and Maynard, H. D. (2008) Reversible siRNA-polymer conjugates by RAFT polymerization. *Chem. Commun. (Camb).* 3245–3247.

(31) York, A. W., Huang, F., and McCormick, C. L. (2010) Rational Design of Targeted Cancer Therapeutics through the Multi-Conjugation of Folate and Cleavable siRNA to RAFT-synthesized (HPMA-s-APMA) Copolymers. *Biomacromolecules 11*, 1–22.

(32) Cho, H. Y., Gao, H., Srinivasan, A., Hong, J., Bencherif, S. a, Siegwart, D. J., Paik, H.-J., Hollinger, J. O., and Matyjaszewski, K. (2010) Rapid cellular internalization of multifunctional star polymers prepared by atom transfer radical polymerization. *Biomacromolecules 11*, 2199–203.

(33) Convertine, A. J., Diab, C., Prieve, M., Paschal, A., Hoffman, A. S., Johnson, P. H., and Stayton, P. S. (2010) pH-Responsive Polymeric Micelle Carriers for siRNA Drugs. *Biomacromolecules 11*, 2904–2911.

(34) Convertine, A. J., Benoit, D. S. W., Duvall, C. L., Hoffman, A. S., and Stayton, P. S. (2009) Development of a novel endosomolytic diblock copolymer for siRNA delivery. *J Control Release 133*, 221–229.

(35) Loczenski Rose, V., Winkler, G. S., Allen, S., Puri, S., and Mantovani, G. (2013) Polymer siRNA conjugates synthesised by controlled radical polymerisation. *Eur. Polym. J. 49*, 2861–2883.

(36) Ardana, A., Whittaker, A. K., McMillan, N. a. J., and Thurecht, K. J. (2015) Polymeric siRNA delivery vectors: knocking down cancers with polymeric-based gene delivery systems. *J. Chem. Technol. Biotechnol. 90*, 1196–1208.

(37) Zhang, Y., Satterlee, A., and Huang, L. (2012) In Vivo Gene Delivery by Nonviral Vectors: Overcoming Hurdles? *Mol. Ther. 20*, 1298–1304.

(38) Ornelas-Megiatto, C., Wich, P. R., and Fréchet, J. M. J. (2012) Polyphosphonium polymers for siRNA delivery: an efficient and nontoxic alternative to polyammonium carriers. *J. Am. Chem. Soc. 134*, 1902–5.

(39) Hemp, S. T., Allen, M. H., Green, M. D., and Long, T. E. (2012) Phosphonium-containing polyelectrolytes for nonviral gene delivery. *Biomacromolecules 13*, 231–8.

(40) Hemp, S. T., Smith, A. E., Bryson, J. M., Allen, M. H., and Long, T. E. (2012) Phosphonium-containing diblock copolymers for enhanced colloidal stability and efficient nucleic acid delivery. *Biomacromolecules 13*, 2439–45.

(41) Qian, C., Xu, X., Shen, Y., Li, Y., and Guo, S. (2013) Synthesis and preliminary cellular evaluation of phosphonium chitosan derivatives as novel non-viral vector. *Carbohydr. Polym. 97*, 676–83.

(42) Chem, J. O., Karaman, H., Barton, R. J., Robertson, B. E., and Lee, D. G. (1984) Preparation and Properties of Quaternary Ammonium and Phosphonium Permanganates. *J Org. Chem. 49*, 4509–4516.

(43) Anderson, E. B., and Long, T. E. (2009) Synthesis and characterization of phosphonium-containing polysulfone ionomers. *Polym. Prepr. 50*, 658–659.

(44) Frank R. Hartley. (1990) The Chemistry of Organophosphorus Compounds, Volume I: Primary, secondary and tertiary phosphines, polyphosphines and heterocyclic organophosphorus (III) compounds.

(45) Perrier, S., Takolpuckdee, P., and Mars, C. a. (2005) Reversible Addition−Fragmentation Chain Transfer Polymerization: End Group Modification for Functionalized Polymers and Chain Transfer Agent Recovery. *Macromolecules 38*, 2033–2036.

(46) Willcock, H., and O'Reilly, R. K. (2010) End group removal and modification of RAFT polymers. *Polym. Chem. 1*, 149–157.

(47) Schneider, C. a, Rasband, W. S., and Eliceiri, K. W. (2012) NIH Image to ImageJ: 25 years of image analysis. *Nat. Methods 9*, 671–675.

(48) Abràmofff, M. D., Magalhães, P. J., and Ram, S. J. (2004) Image processing with ImageJ. *Biophotonics Int. 11*, 36–42.

(49) Ivanov, D. P., Parker, T. L., Walker, D. A., Alexander, C., Ashford, M. B., Gellert, P. R., and Garnett, M. C. (2014) Multiplexing Spheroid Volume, Resazurin and Acid Phosphatase Viability Assays for High-Throughput Screening of Tumour Spheroids and Stem Cell Neurospheres. *PLoS One* (Mancini, M. A., Ed.) *9*, 1–14.

(50) O'Brien, J., Wilson, I., Orton, T., and Pognan, F. (2000) Investigation of the Alamar Blue (resazurin) fluorescent dye for the assessment of mammalian cell cytotoxicity. *Eur. J. Biochem. 267*, 5421–5426.

(51) Moad, G., Chong, Y. K., Postma, A., Rizzardo, E., and Thang, S. H. (2005) Advances in RAFT polymerization: the synthesis of polymers with defined end-groups. *Polymer (Guildf). 46*, 8458–8468.

(52) Moad, G., Rizzardo, E., and Thang, S. H. (2008) Radical addition–fragmentation chemistry in polymer synthesis. *Polymer (Guildf). 49*, 1079–1131.

(53) Perrier, S., and Takolpuckdee, P. (2005) Macromolecular design via reversible addition-fragmentation chain transfer (RAFT)/xanthates (MADIX) polymerization. *J. Polym. Sci. Part A Polym. Chem. 43*, 5347–5393.

(54) Xue, L., Ingle, N. P., and Reineke, T. M. (2013) Highlighting the role of polymer length, carbohydrate size, and nucleic acid type in potency of glycopolycation agents for pDNA and siRNA delivery. *Biomacromolecules 14*, 3903–15.

(55) Yue, Y., Jin, F., Deng, R., Cai, J., Dai, Z., Lin, M. C. . M., Kung, H.-F., Mattebjerg, M. A., Andresen, T. L., and Wu, C. (2011) Revisit complexation between DNA and polyethylenimine - Effect of length of free polycationic chains on gene transfection. *J Control Release. 152*, 143–151.

(56) Nobbmann, U., and Morfesis, A. (2009) Light scattering and nanoparticles. *Mater. Today 12*, 52–54.

(57) Troiber, C., Kasper, J. C., Milani, S., Scheible, M., Martin, I., Schaubhut, F., Küchler, S., Rädler, J., Simmel, F. C., Friess, W., and Wagner, E. (2013) Comparison of four different particle sizing methods for siRNA polyplex characterization. *Eur. J. Pharm. Biopharm. 84*, 255–64.

(58) Fairbanks, B. D., Gunatillake, P. A., and Meagher, L. (2015) Biomedical applications of polymers derived by reversible addition – fragmentation chain-transfer (RAFT). *Adv. Drug Deliv. Rev. 10*, doi: 10.1016/j.addr.2015.05.016.

(59) Siegwart, D. J., Oh, J. K., and Matyjaszewski, K. (2012) ATRP in the design of functional materials for biomedical applications. *Prog. Polym. Sci. 37*, 18–37.

(60) Chehade, M., and Elder, M. J. (1997) Intraocular lens materials and styles: a review. *Aust. N. Z. J. Ophthalmol. 25*, 255–263.

(61) Webb, J. C. J., and Spencer, R. F. (2007) The role of polymethylmethacrylate bone cement in modern orthopaedic surgery. *J. Bone Joint Surg. Br. 89*, 851–857.

(62) Kim, Y. K., Grandini, S., Ames, J. M., Gu, L. S., Kim, S. K., Pashley, D. H., Gutmann, J. L., and Tay, F. R. (2010) Critical Review on Methacrylate Resin-based Root Canal Sealers. *J. Endod. 36*, 383–399.

(63) Htay, T., and Liu, M. W. (2005) Drug-eluting stent: a review and update. *Vasc. Health Risk Manag. 1*, 263–276.

(64) Varkouhi, A. K., Scholte, M., Storm, G., and Haisma, H. J. (2011) Endosomal escape pathways for delivery of biologicals. *J. Control. Release 151*, 220–8.

(65) Patil, M., Zhang, M., Taratula, O., Garbuzenko, O., He, H., and Minko, T. (2009) Internally cationic polyamidoamine PAMAM-OH dendrimers for siRNA delivery: effect of the degree of quaternization and cancer targeting. *Biomacromolecules 10*, 258–266.

(66) Akinc, A., Thomas, M., Klibanov, A. M., and Langer, R. (2005) Exploring polyethylenimine-mediated DNA transfection and the proton sponge hypothesis. *J. Gene Med. 7*, 657–63.

(67) Chang, C. Il, Kim, H. A., Dua, P., Kim, S., Li, C. J., and Lee, D. (2011) Structural diversity repertoire of gene silencing small interfering RNAs. *Nucleic Acid Ther. 21*, 125–31.

(68) Sajeesh, S., and Lee, D. (2015) Advanced Therapeutic Platforms based on Non-Classical Tripodal Interfering RNA Structural Format. *Rna Dis. 2*, 2–5.

(69) Sajeesh, S., Lee, T. Y., Hong, S. W., Dua, P., Choe, J. Y., Kang, A., Yun, W. S., Song, C., Park, S. H., Kim, S., Li, C., and Lee, D.-K. (2014) Long dsRNA-mediated RNA interference and immunostimulation: a targeted delivery approach using polyethyleneimine based nano-carriers. *Mol. Pharm. 11*, 872–84.

(70) Sajeesh, S., Choe, J. Y., Lee, T. Y., and Lee, D. (2014) Guanidine modified polyethyleneimine-g-polyethylene glycol nanocarriers for long interfering RNA (liRNA) based advanced anticancer therapy. *J. Mater. Chem. B Mater. Biol. Med. 3*, 207–216.

(71) Chang, C. Il, Lee, T. Y., Dua, P., Kim, S., Li, C. J., and Lee, D. (2011) Long Interfering Double-Stranded RNA as a Potent Anticancer Therapeutics. *Nucleic Acid Ther. 21*, 149–156.

(72) Chang, C. Il, Lee, T. Y., Yoo, J. W., Shin, D., Kim, M., Kim, S., and Lee, D.-K. (2012) Branched, tripartite-interfering RNAs silence multiple target genes with long guide strands. *Nucleic Acid Ther. 22*, 30–9.

(73) Lee, T. Y., Chang, C. Il, Lee, D., Hong, S. W., Shin, C., Li, C. J., Kim, S., Haussecker, D., and Lee, D.-K. (2013) RNA interference-mediated simultaneous silencing of four genes using cross-shaped RNA. *Mol. Cells 35*, 320–6.